Hindawi Publishing Corporation
Modelling and Simulation in Engineering
Volume 2012, Article ID 671934, 9 pages
doi:10.1155/2012/671934

Research Article

Risk Assessment Method for Offshore Structure Based on Global Sensitivity Analysis

Zou Tao,[1] Li Huajun,[1] and Liu Defu[2]

[1] *College of Engineering, Ocean University of China, Qingdao 266100, China*
[2] *Disaster Prevention Research Institute, Ocean University of China, Qingdao 266003, China*

Correspondence should be addressed to Zou Tao, zt_dream@163.com

Received 4 April 2012; Accepted 27 September 2012

Academic Editor: Agostino Bruzzone

Based on global sensitivity analysis (GSA), this paper proposes a new risk assessment method for an offshore structure design. This method quantifies all the significances among random variables and their parameters at first. And by comparing the degree of importance, all minor factors would be negligible. Then, the global uncertainty analysis work would be simplified. Global uncertainty analysis (GUA) is an effective way to study the complexity and randomness of natural events. Since field measured data and statistical results often have inevitable errors and uncertainties which lead to inaccurate prediction and analysis, the risk in the design stage of offshore structures caused by uncertainties in environmental loads, sea level, and marine corrosion must be taken into account. In this paper, the multivariate compound extreme value distribution model (MCEVD) is applied to predict the extreme sea state of wave, current, and wind. The maximum structural stress and deformation of a Jacket platform are analyzed and compared with different design standards. The calculation result sufficiently demonstrates the new risk assessment method's rationality and security.

1. Introduction

In August 2005, Hurricane Katrina and Rita attacked the coastal areas of the USA and the Gulf of Mexico. Including causing serious damage in New Orleans, it also caused a great loss to petroleum industry in the Gulf of Mexico. According to the incomplete statistic, Katrina and Rita resulted in 116 destroyed and damaged platforms and more than eight oil refineries were forced to cease production. And just in March 11, 2011, a huge earthquake of magnitude 9.0 occurred besides the northeast coast of Japan. The powerful quake sparked the tsunami wave of ten meters in Japan which led to an unexpected nuclear leakage accident. This accident became a death blow to the Japanese economy. Previous studies concluded that a tendency toward the growth of intensity and losses of each disaster is also appearing [1–3]. Most of these disasters resulted from the inaccurate risk assessment of natural hazards. Although natural disasters are dangerous to human, the great loss by each disaster is mainly caused by human's ignorance of disaster prediction. Due to the complexity of the natural events, it is very hard to forecast the occurrence of natural hazards accurately without the global uncertainty analysis (GUA).

In addition, as the law of nature is not clear enough, the design process for offshore structure usually could not predict the real extreme sea state accurately as a result of many kinds of uncertainties. However, because of the great variety of uncertainties, it's not practicable to take all of them into account at the same time. Some uncertainties may have a very small influence on offshore structure design, and some may be hard to calculate by a lack of statistical data. This kind of uncertainty requires a heavy calculating works and the result may not be credible to people. That is why global sensitivity analysis (GSA) is essential for structure design. GSA can quantify the significances among random variables and their parameters. By comparing the degrees of importance, all minor factors would be negligible. In this way, GUA can be totally simplified and the heavy workloads reduced.

Besides the uncertainty factors, all those natural disasters also indicate that the current design criteria have definite defects and deficiencies. The early API practice (1995)

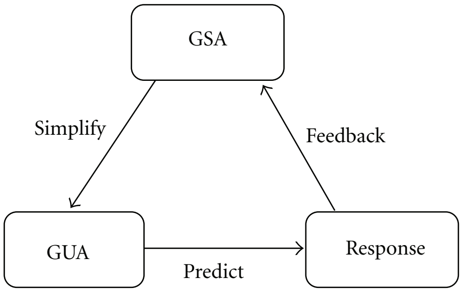

Figure 1: Application of GUA and GSA to structural response.

requires that the design load for fixed platform is 100 yr. return period wave height combined with associated wind and current. According to API, the meaning of "associated" is somewhat ambiguous. Wave, wind, and current are regarded as independent factors, and the combined effect of environment factors is neglected, which lacks scientific principles. Fortunately the API_RP_2A_WSD revised in 2000 rectified this requirement. According to the new edition of API, environment loads, with the exception of earthquake load, should be combined in a manner consistent with the probability of their simultaneous occurrence for the loading condition being considered. Although API (2000) has taken the combination of the environment loads into account, it does not figure out how to use the joint probability theory to analyze, and the effect of different uncertainties in design loads is not considered too. This may result in a hidden peril to the offshore structure design in the future.

In this paper, a new risk assessment method for structural design, which combines GUA with GSA, is proposed. The GSA is made in order to measure the influence of different factors and simplify the GUA. Then the combined effect of environmental loads, sea level, and marine corrosion uncertainties in the structural design stage is studied. At last, different design methods are compared.

2. Global Sensitivity Analysis (GSA)

The main objective of GSA focuses on the influence of failure probability and structural response on random variables and their parameters in the reliability model. It can compare horizontally the significance among random variables and their parameters.

For an output variable y_i, suppose the basic random variables which have influence on the output are $\{x_1, x_2, \ldots, x_i, \ldots, x_n\}$, and E_{x_1} is the expectation of output variable x_i, then the sensitivity vector can be defined as

$$\text{Sensitivity Vector} = \left\{ \frac{\partial y}{\partial x_1} E_{x_1}, \ldots, \frac{\partial y}{\partial x_i} E_{x_i} \ldots, \frac{\partial y}{\partial x_n} E_{x_n} \right\}, \quad (1)$$

which could be described by sensitivity chart after normalization [4].

Global sensitivity analysis is very helpful in dealing with engineering problems. And it could play a guiding role in the area of environmental impact prediction, simulation and assessment, and improve accuracy and reliability of prediction. Based on MCEVD, the global uncertainty analysis (GUA) and global sensitivity analysis (GSA) as main tools can be used for input sea environments with uncertainties and corresponding sensitivity of structure responses. After the simplification of GSA, the structural response calculation works could be greatly reduced; see Figure 1.

This paper takes a Jacket platform with 30 m design depth of water in the South China Sea as an example, and analyzes the global sensitivity of structural stress. In the actual calculation, to clarify the issue, eliminate the influence of structural forms (e.g., stress concentration in tubular joint and green water occurrence) and make the result have general significance, the Jacket is just simplified to a certain extent (see Figure 2).

Based on the finite element model of Ansys, stress sensitivity of Jacket platform is analyzed considering the change of each input variable (wave height, wind velocity, current velocity, section thickness, and sea level, resp.) The sensitivity vector is $\{25.67, 1, 9.17, 17.95, -17.67\}$ and, after normalization, is $\{0.36, 0.01, 0.13, 0.25, 0.25\}$ (see Figure 3).

According to the GSA result, it can be concluded that the sensitivities of different factors vary greatly. Wave height is the most sensitive factor to the Max. stress of platforms, section thickness, and sea level second, current third and wind at last. As the wind sensitivity is very low and current is usually regarded as a fixed value, the GUA of wind and current will not be taken into account. In addition, since sea level's sensitivity is negative, it is not recommended to be used in the calculation for maximum stress.

3. Influence of Global Uncertainty Analysis

3.1. Ocean Environmental Loads. Ocean environmental loads concerning offshore platform design mainly include wave, wind, current, ice, and earthquake. As for the most fixed platforms, wave height is the dominant factor. This paper mainly takes the uncertainty of wave height into account.

3.1.1. Climate Change Uncertainty. Climate change around the world due to greenhouse effects has made a deep influence on human society. The duration of the most extreme events, such as tropical cyclones, is also increasing [2]. So it's very necessary to consider climate change as an uncertainty factor in the process of platform design.

Mori et al. [5] and Yasuda et al. [6] have analyzed the wave change in the Pacific Ocean near southeastern Asia by the General Circulation Model (GCM) and the result indicates that the mean waves will be increased at both the middle latitudes and also in the Antarctic ocean; on the other hand, the extreme waves due to tropical cyclones will be increased as in Figure 4.

According to the wave height data in the South China Sea from 1979 to 1987, the future wave height can be predicted as in Table 1. Hence it is not difficult to obtain the uncertainty of climate change:

$$\text{Cov}_{11} = \frac{\sigma_{11}}{\mu_{11}} = 0.13. \quad (2)$$

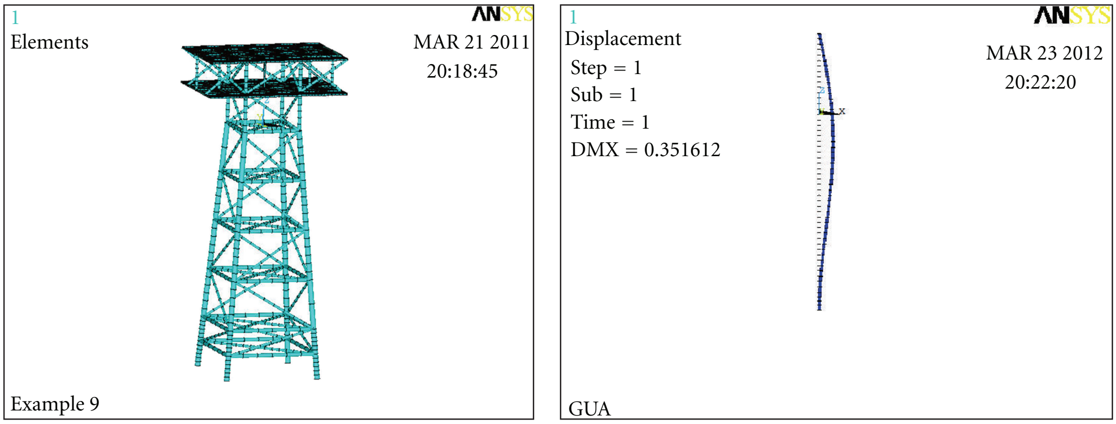

FIGURE 2: The Jacket platform model.

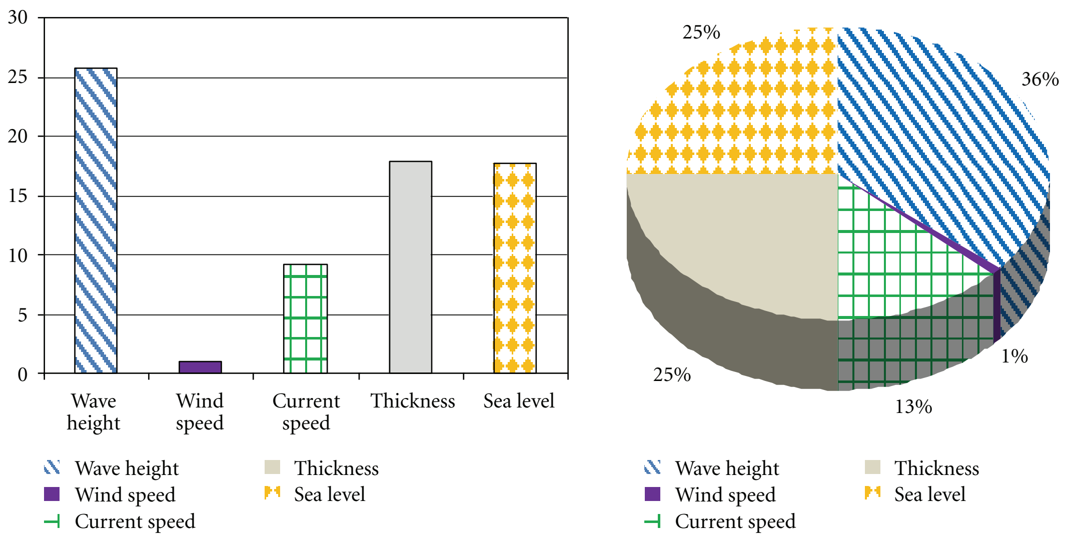

FIGURE 3: Stress Sensitivity of Jacket.

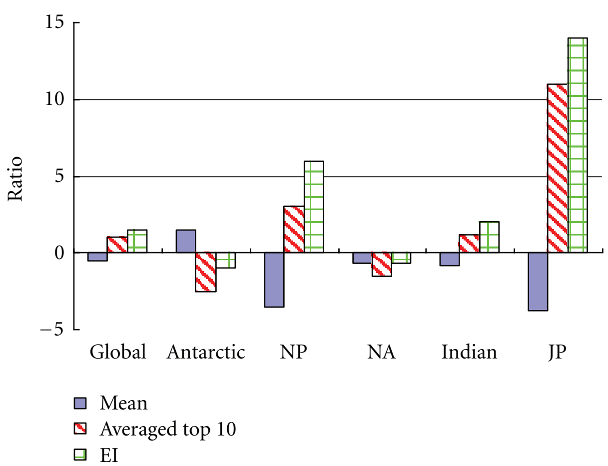

FIGURE 4: Spatially averaged mean, top 10 and EI of Hs (NP: Northern Pacific, NA: Northern Atlantic, JP: Pacific Ocean near Japan).

3.1.2. Method and Model Uncertainty. Sampling with different methods, the result may have a great difference. Some common methods are as follows.

(1) Maximum method: take the maximum value as a sample within a long time return period;

(2) POT method: Peak Over Threshold method: this method would set a threshold value; all the data greater than this value would be taken.

Considering the maximum method and POT method, the sampling result by different method has been made as in Table 2, and the uncertainty is obtained:

$$\mathrm{Cov}_{12} = \frac{\sigma_{12}}{\mu_{12}} = 0.18. \tag{3}$$

3.1.3. Statistical Uncertainty. As the methodology and involved probabilistic models are selected and the corresponding sample is established, the different distribution

Table 1: Wave height data in the South China Sea from 1979 to 1987.

Number	1	2	3	4	5	6	7	8	9	10
Wave height (m)	9.57	13.08	10.89	11.33	11.25	13.53	11.33	11.25	10.23	13.97
Number	11	12	13	14	15	16	17	18	19	20
Wave height (m)	11.48	10.91	13.86	13.42	11.57	11.52	12.98	12.1	11.55	11.06

Table 2: Sampling result by different methods.

Max. (m)	12.8	10.3	12.3	10.3	12.7	7.4	12.6	13.2	11.8	10.5
POT (m)	13.2	12.8	12.7	12.6	12.3	12.2	11.8	11.0	10.5	10.3

Table 3: Prediction result for wave height by different probabilistic models.

Distribution models	Wave height with 100 yr return period (m)
PIII	8.63
GEV	8.83
MCEVD	6.92

models, such as PIII distribution General Extreme Value distribution (GEV) and MCEVD, can be fitted to the data samples. The prediction result for wave height can be seen in Table 3. Since the sample consists of the limited number of realizations, this phase will also be associated with uncertainties. Statistical uncertainty can be obtained as the maximum value:

$$\mathrm{Cov}_{13} = \frac{\sigma_{13}}{\mu_{13}} = 0.14. \tag{4}$$

So resulting global uncertainty of wave height for the South China Sea is:

$$\mathrm{Cov}_{1} = \sqrt{\mathrm{Cov}_{11}^2 + \mathrm{Cov}_{12}^2 + \mathrm{Cov}_{13}^2} = 0.26. \tag{5}$$

3.2. Sea-Level Rise. Because of the greenhouse effect, global warming is raising the temperature by 0.013°C per year which leads to sea level rise at last. According to the latest data, most glaciers around the world suffer a substantial retreat within the coming 50 years in the enhanced greenhouse climate [7]. And sea-level rise has been observed at a rate of 1.7 mm ± 0.3 mm/yr. from 1870 to 2004 [8]. In addition, storm surge and tide may also raise the water level within a short time.

3.2.1. Greenhouse Effect Uncertainty. Based on previous studies, the sea level rising velocity is confirmed as 2.0 mm/yr [9]. Since the design life of the model platform in this paper is 20 years, the uncertainty of greenhouse effect in sea-level rise is

$$\mathrm{Cov}_{21} = \frac{\sigma_{21}}{\mu_{21}} = 0.002. \tag{6}$$

3.2.2. Storm Surge Uncertainty. Based on the statistical data of storm surge in the South China Sea from 1979 to 1987 (see Table 4), the uncertainty of storm surge can be easily confirmed:

$$\mathrm{Cov}_{22} = \frac{\sigma_{22}}{\mu_{22}} = 0.0617. \tag{7}$$

Table 4: Statistical data of storm surge in the South China Sea (1979–1987).

Typhoon number	Surge (m)
7909	0.46
7910	1.09
7915	0.21
7919	0.61
8001	0.18
8002	0.48
8003	0.26
8004	0.41
8101	0.93
8102	0.15
8209	0.52
8211	0.87
8219	0.29
8305	0.27
8310	0.58
8402	0.5
8403	0.15
8406	0.66
8407	0.19
8409	0.77
8504	0.19
8506	0.32
8508	0.24
8519	0.28
8607	0.35
8615	0.49
8617	0.39
8700	0.18
8701	0.26
8704	0.36
8705	0.17
8707	0.43
8711	0.69

Table 5: Calculated spring tide from different inputs.

Input			output
A_n (cm) 1*	$A(M_2)$ (cm) 2*	$A(S_2)$ (cm) 3*	Maximum sea level (cm)
4.08	127.54	41.60	156.12
2.08	123.47	41.53	151.11
−14.92	127.05	40.14	139.62
4.08	126.41	41.39	155.32
20.8	125.22	41.25	152.45
14.92	124.69	41.39	146.41
2.08	124.44	41.22	151.64

Note: 1*: annual mean sea level.
2*: amplitude of constituent M_2.
3*: amplitude of constituent S_2.

Table 6: Corrosion loss by time.

Time (yr)	1	2	3	4	5	6	7	8
Loss (mm)	0.18	0.30	0.36	0.42	0.48	0.54	0.59	0.65
Time (yr)	9	10	11	12	13	14	15	16
Loss (mm)	0.71	0.77	0.83	0.88	0.94	1.00	1.06	1.12
Time (yr)	17	18	19	20	21	22	23	24
Loss (mm)	1.17	1.23	1.29	1.35	1.41	1.47	1.52	1.58

3.2.3. Spring Tide Uncertainty. Because tide has its own law of motion, the periodical change is fluctuated by some other factors such as geographical reasons [10]. The spring tide height can be combined by different constituents as in Table 5, and the astronomical tide uncertainty can be obtained:

$$\mathrm{Cov}_{23} = \frac{\sigma_{23}}{\mu_{23}} = 0.0817. \tag{8}$$

So the resulting global uncertainty of sea-level rise for the South China Sea is

$$\mathrm{Cov}_2 = \sqrt{\mathrm{Cov}_{21}^2 + \mathrm{Cov}_{22}^2 + \mathrm{Cov}_{23}^2} = 0.1024. \tag{9}$$

3.3. Marine Corrosion. For offshore structures, Jacket part is inevitably exposed to air and sea water at the same time, which may lead to a serious marine corrosion. And as known to all, the structural resistance would definitely be reduced by the loss of section thickness. See Figure 5. Although the designer may take marine corrosion into account, there are also some other uncertainties in the corrosion rate.

3.3.1. Design Life Uncertainty. According to various coupon tests and observations, the material loss due to corrosion can be seen as a function of time [11]. The corrosion model feature is shown in Figure 6. Sometimes, offshore platforms need to keep producing after the design life, just like when the oil wells are not exhausted. In this case, the design life is lengthened. In this paper, the design life of platform is 20 yr and it has a 4 more years working requirement (see Table 6). Then, based on the corrosion model feature, the design life uncertainty can be gotten:

$$\mathrm{Cov}_{31} = \frac{\sigma_{31}}{\mu_{31}} = 0.2153; \tag{10}$$

$$\begin{aligned} r_0 &= 0.076\exp(0.054T); & t_a &= 6.61\exp(-0.088T); \\ c_a &= 0.32\exp(-0.038T); & r_a &= 0.066\exp(0.061T); \\ c_s &= 0.075 + 5678T^{-4}; & r_s &= 0.045\exp(0.017T); \end{aligned} \tag{11}$$

T is the average seawater temperature.

3.3.2. Water Velocity Uncertainty. The velocity of water may influence the marine corrosion rate. The widely accepted work in this area is made by LaQue. Figure 7 and Table 7 show the corrosion results at 20°C and the uncertainty of water velocity would be

$$\mathrm{Cov}_{32} = \frac{\sigma_{32}}{\mu_{32}} = 0.50. \tag{12}$$

3.3.3. Pollution Uncertainty. The effect of pollution can be obtained simply from considering the influence of environmental pollution. In fact, many events can lead to a serious water pollution such as oil spill or agricultural and industrial wastewater discharge [12]; see Figure 8 and Table 8. Considering the measurement by Robert E. Melchers, the pollution uncertainty is

$$\mathrm{Cov}_{33} = \frac{\sigma_{33}}{\mu_{33}} = 0.6154. \tag{13}$$

So global uncertainty of marine corrosion is

$$\mathrm{Cov}_3 = \sqrt{\mathrm{Cov}_{31}^2 + \mathrm{Cov}_{32}^2 + \mathrm{Cov}_{33}^2} = 0.8216. \tag{14}$$

4. Prediction of Extreme Environmental Loads

This example applied 143 typhoons of the Dapeng Bay and selects the wind velocity, wave height, and current velocity of each process as samples. Based on the diagnose tests and Kolmogorov-Smirnov inspection, the sample points and the curves of general extreme value (GEV) distribution fit well. The location parameter μ, scale parameter σ, and shape parameter ξ are estimated in Table 9.

According to the diagnose figure, the confidence level of the sample all falls between 95% confidential interval. In order to avoid repetition, only the diagnose figure of wave height (H) is showed in Figure 9, similar to wind velocity (V) and current velocity (C).

5. Multivariate Compound Extreme Value Distribution

The theory of Compound Extreme Value Distribution (CEVD) was first proposed by Liu and Ma in 1980 [13].

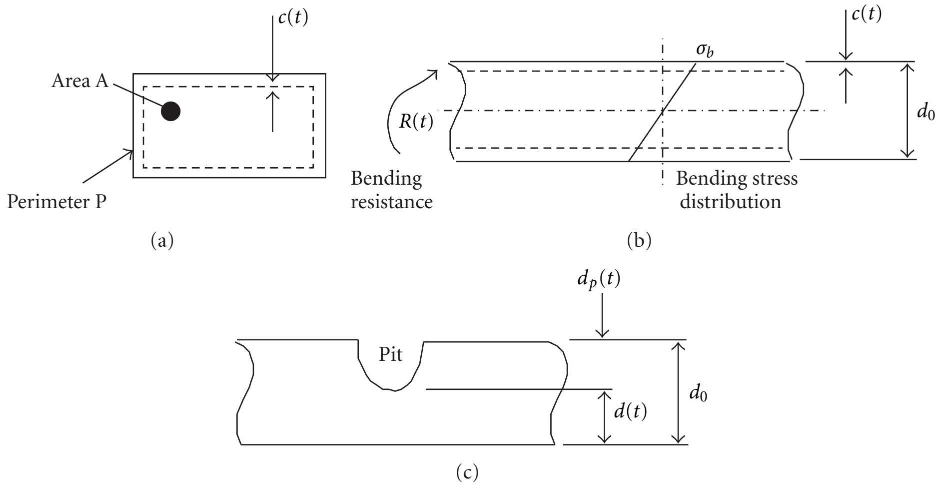

FIGURE 5: (a) Cross-section of a bar under axial stress showing corrosion loss, (b) cross-section of a plate under bending stress showing effect of corrosion, and (c) cross-section of a plate subject to pitting from one side, σd_o.

TABLE 7: Effect of different water velocities on corrosion loss.

Time (day)	80	100	120	160	200	240	280	320
0.35 m/s	45 μm	60 μm	70 μm	85 μm	110 μm	125 μm	150 μm	170 μm
0.45 m/s	60 μm	80 μm	100 μm	125 μm	150 μm	175 μm	200 μm	220 μm
Difference	15 μm	20 μm	30 μm	40 μm	40 μm	50 μm	50 μm	50 μm

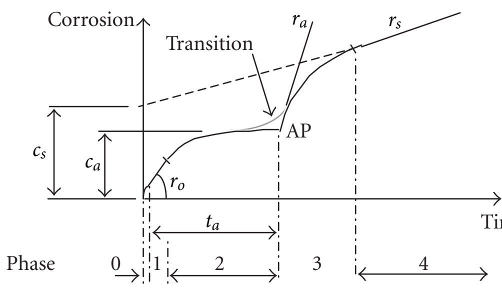

FIGURE 6: Corrosion model.

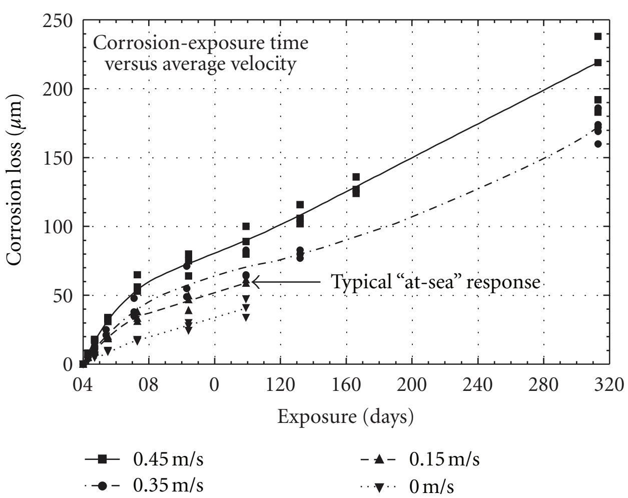

FIGURE 7: Effect of water velocity on corrosion loss [12].

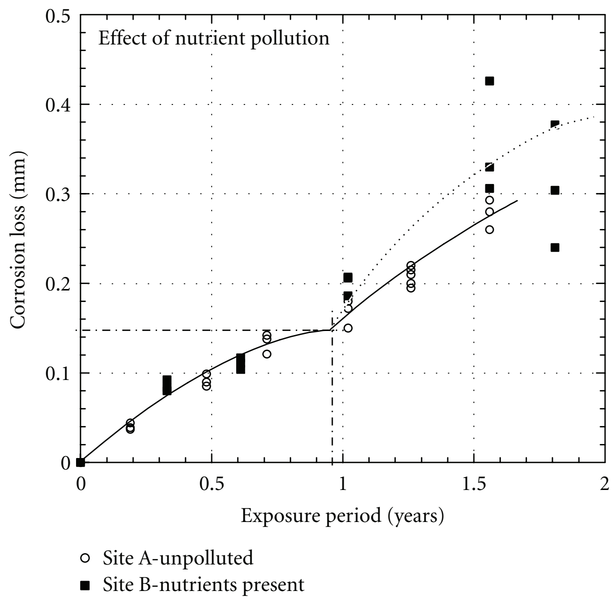

FIGURE 8: Corrosion loss period of exposure curves for two similar sites, with site B found to have a high nutrient level [12].

TABLE 8: Comparison by polluted and unpolluted sites.

Time (yr)	0.5	1	1.5	2
Unpolluted site	0.10 mm	0.15 mm	0.26 mm	0.34 mm
Polluted site	0.10 mm	0.15 mm	0.32 mm	0.42 mm

Table 9: Parameters of variables.

	Shape parameter ξ	Scale parameter σ	Location parameter μ	Dn	Dn (0.05)
H (m)	0.1655	0.9630	2.1907	0.0604	0.1123
V (m/s)	−0.6084	8.2255	34.4579	0.1512	0.2941
C (m/s)	−0.3314	0.4525	1.3346	0.0918	0.2941

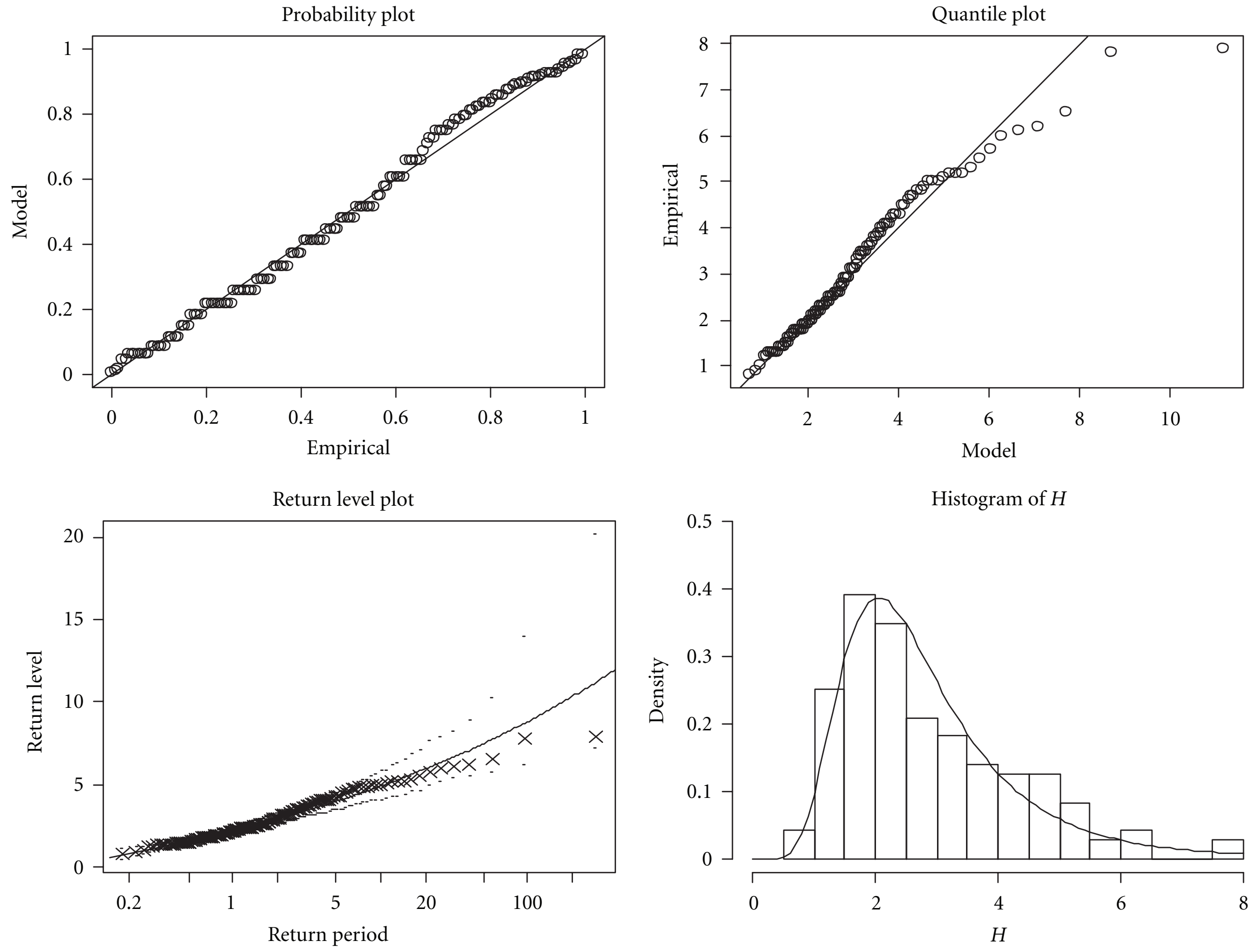

Figure 9: Diagnostic checks of H.

During the past few years, CEVD has been developed into MCEVD and applied to predict multivariate joint probability [14]. The expression of MCEVD can be described by (15):

$$P(\lambda; x_1, x_2, \ldots x_n) = e^{-\lambda}\left(1+\iint_{\Omega}\cdots\int e^{\lambda F(x)} f(x_1, x_2, \ldots x_n)dx_1 dx_2 \cdots dx_n\right), \quad (15)$$

in which λ is the mean value of the annual typhoon frequency; Ω is joint probability domain; $f(\cdot)$, $F(\cdot)$ are the probability density function and cumulative function; $x_1, x_2, \ldots x_n$ are random variables such as typhoon characteristics: ΔP, Rmax, s, δ, θ, and t.

When the dimension $n \leq 3$, (15) can be solved by the analytical method. When $n > 3$, finding theory solution will become unpractical, the Stochastic Simulation Method (SSM) should be used to solve MCEVD.

When the trivariate nested logistic model can be involved into (15), then Poisson Nested Logistic Trivariate Compound Extreme Value Distribution (PNLTVEVD) can be derived as a practically useful model of MCEVD [15]. The PNLTCED can be obtained from (16):

$$F_0(x_1, x_2, x_3) = e^{-\lambda}\left(1+\lambda\int_{-\infty}^{x_3}\int_{-\infty}^{x_2}\int_{-\infty}^{x_1} e^{\lambda\cdot F(u_1)} f(u_1, u_2, u_3)du_1 du_2 du_3\right). \quad (16)$$

Table 10: Comparison of calculated results by different definitions.

	Wave (m)	Wind (m/s)	Current (m/s)	Sea level (m)	Section thickness (mm)	Max. DOF (m)	Max. stress (Pa)	Joint return period (yr)
API	8.63	39.90	1.24	0	25.4	0.3088	0.118$e+9$	150
GUA	8.72	45.86	1.50	3	22.9	0.3507	0.124$e+9$	180
GUA and GSA	8.72	45.86	1.50	0	22.9	0.3516	0.133$e+9$	185

DOF: degree of freedom, representing the displacement of structure.

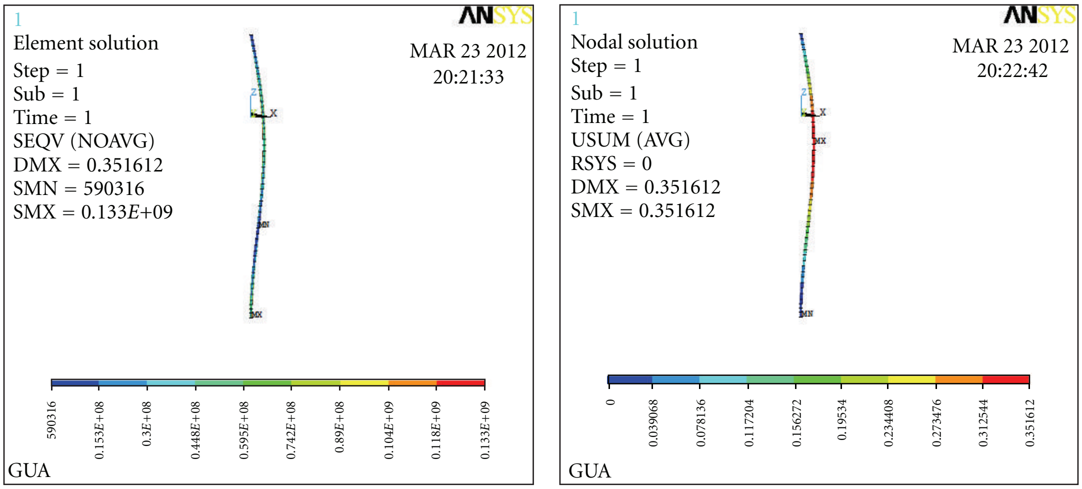

Figure 10: Stress and deformation of Jacket.

in which the cumulative distribution function of trivariate nested logistic model is expressed as

$$F(x_1,x_2,x_3) = \exp\left[-\left\{\left[\left(1+\xi_1\frac{x_1-\mu_1}{\sigma_1}\right)^{-1/\alpha\beta\xi_1} + \left(1+\xi_2\frac{x_2-\mu_2}{\sigma_2}\right)^{-1/\alpha\beta\xi_2}\right]^{\beta} + \left(1+\xi_3\frac{x_3-\mu_3}{\sigma_3}\right)^{-1/\alpha\xi_3}\right\}^{\alpha}\right],$$

$$f(x_1,x_2,x_3) = \frac{\partial^3 F(x_1,x_2,x_3)}{\partial x_1 \partial x_2 \partial x_3} \tag{17}$$

in which ξ_j, μ_j, σ_j are the shape, location, and scale parameters of marginal distributions $F(x_j)$ to x_j $(j = 1,2,3)$, respectively. And dependent parameters α, β can be obtained through moment estimation

$$\hat{\alpha} = \frac{\sqrt{1-r_{13}} + \sqrt{1-r_{23}}}{2}, \quad \hat{\beta} = \frac{\sqrt{1-r_{12}}}{\hat{\alpha}}, \tag{18}$$

where $r_{i,j}$ is the correlation coefficient, $i < j$, $i,j = 1,2,3$.

Trivariate layer structure (α-outside, β-inside layer) shows that the correlation between x_1 and x_2 is stronger than that among x_1, x_3 and x_2, x_3.

6. Application of MCEVD and Global Uncertainty Analysis (GUA)

Comparing different design load standards, this paper gives three definitions about the design extreme loads, takes a Jacket platform with 30 m design depth of water in the South China Sea as an example, and analyzes the maximum structural stress and deformation with different design standards. The result is showed in Table 10 and Figure 10.

(1) API design method: 100 yr. return period wave height combined with associated wind and current. The 100 yr. return period wave height is usually calculated by fitting Pearson-III curves.

(2) GUA design method: owing to MCEVD model, this method considers the correlation among the factors and takes the simultaneous wave, wind, and current as design criteria. And based on GUA, 100 year sea state is defined by taking account of the influence of wave change and other uncertainty factors (marine corrosion and sea level), so it can give the real "100 year" sea state.

(3) GSA and GUA design method: By GSA, the global uncertainty analysis is simplified. Only wave height

and marine corrosion are regarded as main uncertainty factors. Other uncertainties are negligible. This method is also based on MCEVD model.

MCEVD considers both the frequency and the correlation among the sea environment events. In the 100 yr return period extreme sea state predicted by MCEVD, both wind and current speed are greater than API method, and, on the other hand, wave height (6.92 m) is relatively lower. However, after global uncertainty analysis, wave height, wind and current velocity are all greater than API method. So it indicates that the extreme design loads by traditional API method are underestimated. The global uncertainty analysis is quite necessary. In addition, after the simplification of GSA, GSA and GUA method could reduce the total calculation works and also make a relatively accurate result.

7. Conclusions

Faced with the increasing trend of natural disasters, this paper proposed a new method for risk assessment of offshore structures. The following results sufficiently demonstrate proposed method's rationality and security.

(1) In the 100 yr return period extreme sea state predicted by MCEVD, both wind and current speed are greater than API method, and, on the other hand, wave height is relatively lower. However, considering the influence by the uncertainty of wave, the wave height becomes higher than API method and the joint return period reaches 180 yr. So it indicates that the extreme design loads given by API traditional method is underestimated. And the analysis result of a Jacket platform also shows that both Max. DOF and stress are greater than API method.

(2) The difference between the results of analysis with GUA and GUA and GSA methods is very small. That proves that it is not necessary to take other minor uncertainty factors into account in platform design and GSA is very helpful in simplifying the GUA.

(3) The Max. DOF and Stress of GUA and GSA method is a little greater than GUA method. That's because the sensitivity of the rise of sea level is negative (sea-level rise may lead to the occurrence of green water on the platform deck, but this paper does not consider this effect). For the analysis of extreme loads for the Jacket part, it is not recommended to calculate sea rise. Due to the lack of statistical data, many other uncertainty factors, such as ice or earthquake, are not considered, which may require a deeper research.

Acknowledgments

This work is supported by the National Natural Foundation of China (no. 51010009) and 973 Program (2011CB013704).

References

[1] X. L. Wang, Y. M. Wang, F. M. Ren, and W. J. Li, "Interdecadal variations in frequencies of typhoons affecting china during 1951–2004," *Advances in Climate Change Research*, vol. 3, pp. 66–69, 2007.

[2] G. Rozynski, "The rise of extreme typhoon power and duration over south east Asia seas," *Coastal Engineering Journal*, pp. 205–222, 2009.

[3] K. Walsh, "Tropical cyclones and climate change: unresolved issues," *Climate Research*, vol. 27, no. 1, pp. 77–83, 2004.

[4] W. Z. Fang, "An analysis of structure sensitivity of Ansys PDS," *Journal of East China Jiaotong University*, vol. 27, no. 1, pp. 17–21, 2010.

[5] N. Mori, T. Yasuda, H. Mase, T. Tom, and Y. Oku, "Projection of extreme wave climate change under global warming," *Hydrological Research Letters*, vol. 4, pp. 15–19, 2010.

[6] T. Yasuda, H. Mase, and N. Mori, "Projection of future typhoons landing on Japan based on a stochastic typhoon model utilizing AGCM projections," *Hydrological Research Letters*, vol. 4, pp. 65–69, 2010.

[7] C. Schneeberger, H. Blatter, A. Abe-Ouchi, and M. Wild, "Modelling changes in the mass balance of glaciers of the northern hemisphere for a transient $2\times CO_2$ scenario," *Journal of Hydrology*, vol. 282, no. 1–4, pp. 145–163, 2003.

[8] M. Hemer, J. Church, V. Swail, and X. Wang, "Coordinated global wave climate projections," *Atmosphere-Ocean Interactions*, vol. 2, pp. 185–218, 2006.

[9] J. Church and N. White, "A 20th century acceleration in global sea-level rise," *Geophysical Research Letters*, vol. 33, Article ID L01602, 4 pages, 2006.

[10] B. T. Xie, D. F. Liu, H. J. Li, and C. Gong, "Design code calibration of offshore platform against typhoon/hurricane attacks," *China Ocean Engineering*, vol. 24, no. 3, pp. 431–442, 2010.

[11] M. Q. Zhang, M. Beer, S. T. Quek, and Y. S. Choo, "Comparison of uncertainty models in reliability analysis of offshore structures under marine corrosion," *Structural Safety*, vol. 32, no. 6, pp. 425–432, 2010.

[12] R. E. Melchers, "The effect of corrosion on the structural reliability of steel offshore structures," *Corrosion Science*, vol. 47, no. 10, pp. 2391–2410, 2005.

[13] L. Teh-Fu and M. Feng-Shi, "Prediction of extreme wave heights and wind velocities," *Journal of the Waterway, Port, Coastal and Ocean Division*, vol. 106, no. 15862, pp. 469–479, 1980.

[14] D. Liu, L. Wang, and L. Pang, "Theory of multivariate compound extreme value distribution and its application to extreme sea state prediction," *Chinese Science Bulletin*, vol. 51, no. 23, pp. 2926–2930, 2006.

[15] D. Liu, L. Pang, B. Xie, and Y. Wu, "Typhoon disaster zoning and prevention criteria—a double layer nested multi-objective probability model and its application," *Science in China, Series E*, vol. 51, no. 7, pp. 1038–1048, 2008.

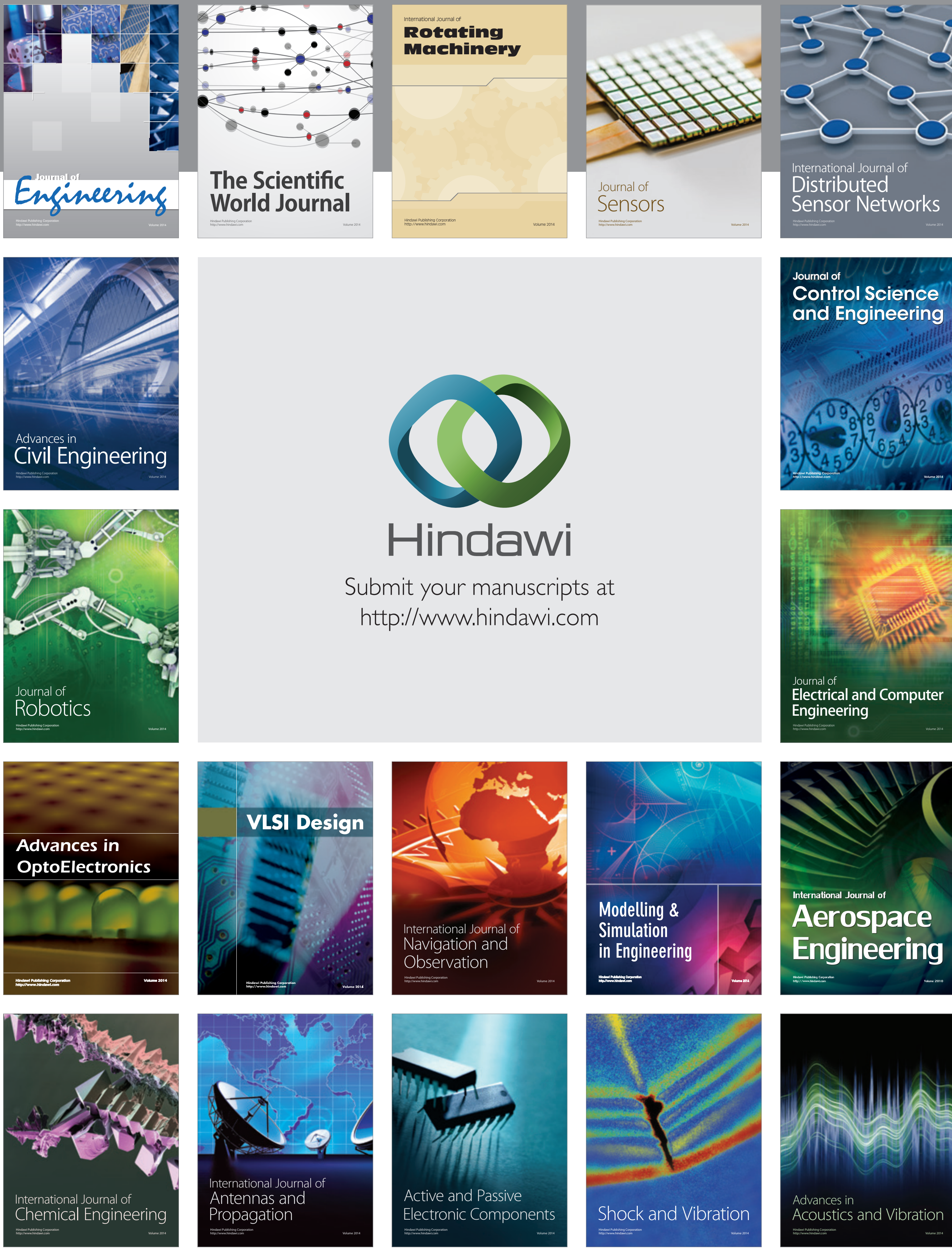
Journal of Engineering
The Scientific World Journal
International Journal of Rotating Machinery
Journal of Sensors
International Journal of Distributed Sensor Networks
Advances in Civil Engineering
Journal of Control Science and Engineering
Hindawi
Submit your manuscripts at
http://www.hindawi.com
Journal of Robotics
Journal of Electrical and Computer Engineering
Advances in OptoElectronics
VLSI Design
International Journal of Navigation and Observation
Modelling & Simulation in Engineering
International Journal of Aerospace Engineering
International Journal of Chemical Engineering
International Journal of Antennas and Propagation
Active and Passive Electronic Components
Shock and Vibration
Advances in Acoustics and Vibration